JACS
JOURNAL OF THE AMERICAN CHEMICAL SOCIETY
Article
pubs.acs.org/JACS

First-Principles Study of the Role of Interconversion Between NO_2, N_2O_4, *cis*-ONO-NO_2, and *trans*-ONO-NO_2 in Chemical Processes

Wei-Guang Liu and William A. Goddard, III*

Materials and Process Simulation Center, California Institute of Technology, Pasadena, California 91125, United States

Supporting Information

ABSTRACT: Experimental results, such as NO_2 hydrolysis and the hypergolicity of hydrazine/nitrogen tetroxide pair, have been interpreted in terms of NO_2 dimers. Such interpretations are complicated by the possibility of several forms for the dimer: symmetric N_2O_4, *cis*-ONO-NO_2, and *trans*-ONO-NO_2. Quantum mechanical (QM) studies of these systems are complicated by the large resonance energy in NO_2 which changes differently for each dimer and changes dramatically as bonds are formed and broken. As a result, none of the standard methods for QM are uniformly reliable. We report here studies of these systems using density functional theory (B3LYP) and several ab initio methods (MP2, CCSD(T), and GVB-RCI). At RCCSD(T)/CBS level, the enthalpic barrier to form *cis*-ONO-NO_2 is 1.9 kcal/mol, whereas the enthalpic barrier to form *trans*-ONO-NO_2 is 13.2 kcal/mol, in agreement with the GVB-RCI result. However, to form symmetric N_2O_4, RCCSD(T) gives an unphysical barrier due to the wrong asymptotic behavior of its reference function at the dissociation limit, whereas GVB-RCI shows no barrier for such a recombination. The difference of barrier heights in these three recombination reactions can be rationalized in terms of the amount of B_2 excitation involved in the bond formation process. We find that the enthalpic barrier for N_2O_4 isomerizing to *trans*-ONO-NO_2 is 43.9 kcal/mol, ruling out the possibility of such an isomerization playing a significant role in gas-phase hydrolysis of NO_2. A much more favored path is to form *cis*-ONO-NO_2 first then convert to *trans*-ONO-NO_2 with a 2.4 kcal/mol enthalpic barrier. We also propose that the isotopic oxygen exchange in NO_2 gas is possibly via the formation of *trans*-ONO-NO_2 followed by ON^+ migration.

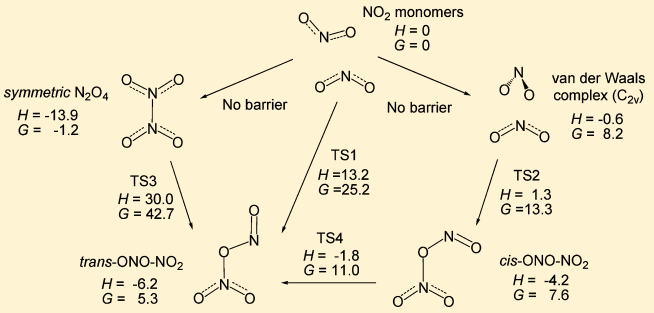

1. INTRODUCTION

Nitrogen dioxide (NO_2) plays an important role in different branches of chemistry. Liquid NO_2 dimerizes to form N_2O_4 (also called nitrogen tetroxide, NTO) and serves as a multifunctional agent for organic synthesis[1] (useful in nitration, nitrosation, and oxidation) and an oxidizer of hypergolic fuel.[2] In atmosphere, NO_2 can react with water vapor to give HONO, a major atmospheric OH source when photolyzed.[3] In addition to the hydrolysis, NO_2 can react with HCl to give ClNO, a potentially harmful gas that photolyzes to form a chlorine atom, an important species in atmospherical chemistry.[4,5]

In many cases with NO_2 as reactant, it is not NO_2 monomer itself that directly participates reactions, but via its asymmetric dimer, ONO-NO_2. Koda et al.[6] proposed that the reaction between NO_2 and methanol in gas phase may go through the asymmetric dimer to give HONO and CH_3ONO_2. Finlayson-Pitts and co-workers[7] proposed that the asymmetric dimer on surfaces plays an key role in NO_2 hydrolysis to form HONO and HNO_3. Raff et al.[4] and Njegic et al.[5] found low-barrier pathways for ONO-NO_2 reacting with HCl to give ClNO. Lai et al.[53] proposed that the hypergolicity of hydrazine/NTO mixture may relate to the asymmetric dimer in NTO. With their chemical importance, however, the pathways forming of such asymmetric isomers and their interconversion have not been fully understood.

NO_2 is a radical which in the valence bond (VB) description involves a resonance of the three configurations A−C shown in Figure 1 that combine to form the ground state. Here each atom is neutral, and the curved solid lines in A and B indicate spin paired π bonds, while the curved dashed line in C indicates the four-electron three-center π bond, as in the ozone ground state. Often the neutral diagram C is written as the superposition of the zwitterion states shown in D and E. In the molecular orbital (MO) description, the singly occupied molecular orbital (SOMO) is a combination of the three singly unpaired orbitals in A−C to give the a_1 SOMO.

From the VB diagrams in Figure 1, we see that there are several ways to spin pair the orbitals of two NO_2 radicals to make a closed-shell dimer. But as shown in Figures 2 and 3, each such case must lose some of the ABC resonance stabilization in Figure 1. This dramatically weakens the new bond and can lead to a barrier for dimerization. Here we can form:

- N−N bond leading to symmetric N_2O_4 as in Figure 2A

Received: January 17, 2012
Published: July 11, 2012

   dx.doi.org/10.1021/ja300545e | J. Am. Chem. Soc. 2012, 134, 12970−12978

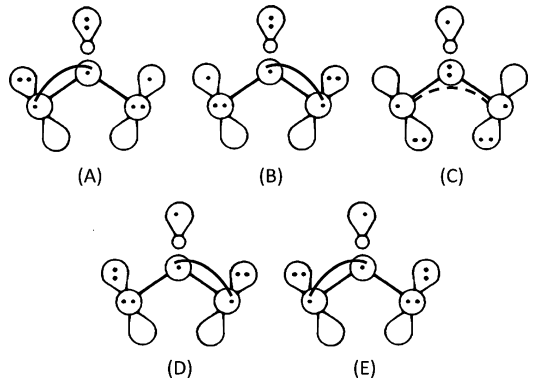

Figure 1. GVB diagrams for NO_2. (A–C) Three VB diagrams for NO_2 that combine to form the ground state. Here each atom is neutral, and the curved solid lines in (A,B) indicate spin paired π bonds, while the curved dashed line in (C) indicates the four-electron three-center π bond, as in the ozone ground state. Often the neutral diagram (C) is written as the superposition of the zwitterion states shown in (D,E).

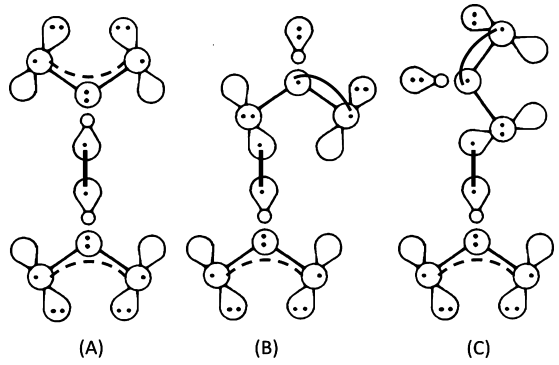

Figure 2. GVB diagrams for N–N and N–O dimers. (A) N–N bond case leading to NTO. (B,C) The *cis* (*endo*) and *trans* (*exo*) asymmetric dimers for the N–O bond case.

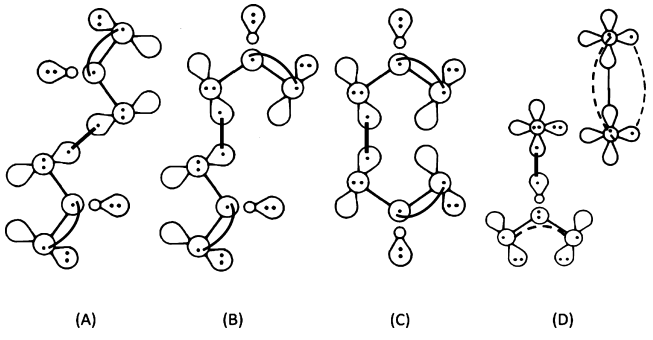

Figure 3. GVB diagrams for (A–C) O–O dimers and (D) $NO^+NO_3^-$ ionic pair.

- N–O bond leading to *endo* or *cis*-ONO-NO_2, and *exo* or *trans*-ONO-NO_2 as in Figure 2B,C
- O–O bond leading to three types of conformations of ONO-ONO isomers[8–13] as in Figure 3A–C
- zwitterion or ion pair $NO^+NO_3^-$ shown in Figure 3D[14]

Among these, N_2O_4 (symmetric dimer) is most stable, with properties that have been measured in both gas and condensed phases. The asymmetric dimer, ONO-NO_2, is less stable, but its existence in the condensed phase has been identified via IR spectroscopy.[15–24] Density functional theory (DFT) at B3LYP level suggests that three ONO-ONO isomers are highly unstable (about 35 kcal/mol higher than N_2O_4),[14,25] because forming the weak O–O bond does not compensate the loss of the resonance energy for each monomer, making them of little chemical importance in ambient conditions if NO_2 is the only reactant. However, such ONO-ONO isomers can be important intermediates in the NO oxidation process.[25–27] Breaking the middle O–O bond leads to the final oxidation product, NO_2.

Several ab initio studies have been carried out for reactions between different isomers of NO_2 and water. Chou et al.[28] performed a DFT study, showing that the energy barrier for N_2O_4 to react with a single H_2O molecule is 32.1 kcal/mol. Njegic et al.[5] found that the activation energy for *cis*-ONO-NO_2 reacting with H_2O is only 8.7 kcal/mol (at the CCSD(T)/cc-pVTZ level). Zhu et al. found the enthalpic barrier of hydrolysis for *cis*-ONO-NO_2 is 10.2 kcal/mol and for *trans*-ONO-NO_2 is 6.4 and 8.0 kcal/mol at CCSD(T)/6-311++G(3df,2p) level.[29] The much lower barriers for asymmetric ONO-NO_2 dimer reacting with water reflect their importance in NO_2 hydrolysis.

To determine the mechanism for the formation of asymmetric ONO-NO_2, Pimentel et al.[30] used DFT (B3LYP) with the polarizable continuum model (PCM) to determine the potential energy surface (PES) of N_2O_4 isomerizing to ONO-NO_2. They reported a free energy barrier of 31.3 kcal/mol (gas phase) and 21.1 kcal/mol (in water). They also reported there to be no enthalpic barrier for two NO_2 to form *trans*-ONO-NO_2.[31] Gadzhiev et al.[25,27] explored possible reactions in NO oxidation, including the isomerization between *cis* and *trans* isomers and dissociation of these isomers. Unlike the previous work, they reported that activation energies for *cis*- and *trans*-ONO-NO_2 dissociation into two NO_2 are 0.43 and 17.0 kcal/mol, respectively, at CAS(26e,16o)/cc-pVDZ level. The attempt to locate the exact transition state (TS) for the dissociation of ONO-NO_2 isomers was not successful with CCSD(T). Very recently, a CAS(12e, 9o)/CASPT2 calculation was carried out for the formation of N_2O_4 and *trans*-$ONONO_2$, giving the former no barrier and the latter 17.1 kcal/mol barrier.[32]

In addition to PES studies, some dynamic simulations have been performed to study the interconversion of these isomers. Miller et al.[33] used second-order Møller–Plesset perturbation theory (MP2) in molecular dynamics (MD) simulations of the autoionization of *cis*- and *trans*-ONO-NO_2 in water clusters, suggesting that ONO-NO_2 dissociates into NO^+ and NO_3^- rapidly when there are more than three water molecules in the cluster. Medeiros and Pimentel[34] also conducted a MD simulation using B3LYP forces, observing that two NO_2 can dimerize into N_2O_4, ONO-NO_2, and even ONO-ONO when less than four water molecules are present explicitly.

Although suggestive, the accuracy of these potentials used in the MD studies to describe these reactions has not been fully validated. The only reaction studied using high-level ab initio methods is $2NO_2 \rightarrow N_2O_4$, and even here the result is controversial. MRCI(15o,16e)/aug-cc-pVDZ[35] and CASSCF (12o,18e)/cc-pVTZ[36] showed no barrier for this recombination, whereas RCCSD(T)/cc-pVTZ leads to a 4.1 kcal/mol barrier.[36]

Calculating the full PES for interactions of two multicenter free radicals requires more care for both post-Hartree–Fock and DFT methods. For post-Hartree–Fock methods, a multireference wave function is necessary to properly describe the transition from open-shell character at large separations to closed-shell singlet at small separations. Thus the CCSD(T) method with a single RHF reference function fails to describe

dx.doi.org/10.1021/ja300545e | J. Am. Chem. Soc. 2012, 134, 12970–12978

bond dissociation, leading to a false barrier for the formation process for many cases, even for F_2.[37] DFT leads to similar problems for calculating the PES for dissociation because of the single Slater determinant formalism. It is particularly important to understand these limitations for systems with both important static and dynamic correlations, as for NO_2 isomers.

In this study we investigated the interconversion of five forms of dinitrogen tetroxide isomers: two free NO_2 molecules, symmetric N_2O_4 dimer, *trans*- and *cis*-ONO-NO_2, and its precursor, the van der Waals complex with C_{2v} symmetry, as shown in Scheme 1, aiming to answer the following questions:

Scheme 1. Reaction Paths and Thermochemical Data for Interconversion between Isomers of Dinitrogen Tetroxide[a]

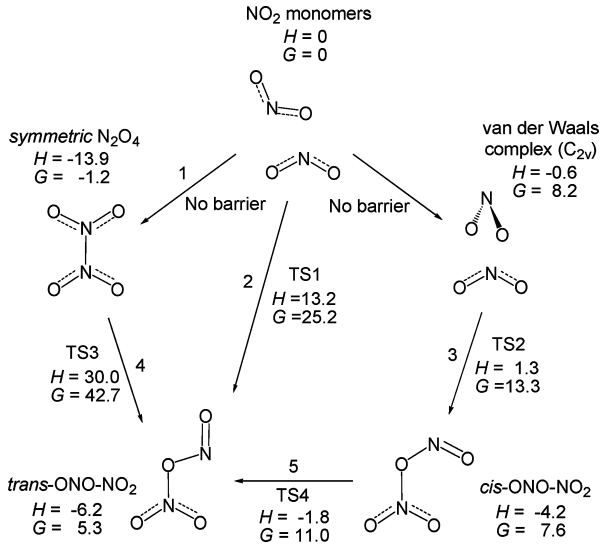

[a]At RCCSD(T)/CBS level and NTP condition except the van der Waals complex, see text. Enthalpy and free energy are in kcal/mol.

- In which cases does the dimerization of NO_2 have barriers?
- In the NO_2 hydrolysis mechanism proposed by Finlayson-Pitts et al., the isomerization of symmetric N_2O_4 to asymmetric ONO-NO_2 is the key step. However this step has been shown to have a 31.3 kcal/mol free energy barrier in gas phase.[30] It has been suggested that the formation of asymmetric dimer is via *cis*-$ONONO_2$ and then isomerizes into *trans*-$ONONO_2$,[24,27] however accurate barrier heights are still undetermined.
- Olson et al.[26] showed that the conformation of ONO-ONO isomer (*cis*−*cis*, *cis*−*trans*, and *trans*−*trans*) drastically affects the barrier for cleavage of the O−O bond. They postulated that −ONO fragment(s) in *cis* orientation would dissociate on the PES of A_1 ground state whereas the one(s) in trans orientation would dissociate with B1 character(excited state), leading to a higher barrier. Such a state-dependent dissociation was also proposed for the isomerization between *trans*-FONO and FNO_2.[38] Asymmetric *cis*- and *trans*-ONO-NO_2 in this system provide another good model system for demonstrating such a state-dependent association and dissociation. It would be interesting to compare all these various reactions of NO_2, which leads to the following question: Can we have a direct and quantitative indicator to define whether a reaction is state dependent or not?

To compare the methods used in the literature, we applied several different QM methods, including DFT with the B3LYP functional, MP2, coupled-cluster singles and doubles with perturbative connected triples (CCSD(T)), and generalized valence bond (GVB) followed by restricted configuration interaction (GVB-RCI). Each method has its own advantages and disadvantages, with none being totally satisfactory. B3LYP is widely used and has been applied on most previous theoretical studies of these systems. MP2 is the first step in going beyond Hartree−Fock to include the electron correlation and is one of few post-Hartree−Fock methods that provide analytical gradient for MD studies.

CCSD(T) incorporates dynamic correlation quite well and can be the most reliable method for closed-shell species in this study. Since an unrestricted Slater determinant can approach the correct dissociation limit, it might give a reasonable PES. Thus for MP2 and CCSD(T), we compared the use of restricted and unrestricted Hartree−Fock wave functions as the reference. GVB is the simplest multireference method that allows smooth transition from closed- to open-shell configuration. It naturally accounts for the static correlation important in the bond-breaking processes; but GVB deliberately ignores dynamic correlation (to obtain a one-electron picture of bonding). To compensate for this, we include a restricted CI among the GVB orbitals (GVB-RCI) to include effects of resonance and spin couplings plus dynamic correlation within the bond pair. GVB-RCI is expected to provide an unbiased PES through the entire dissociation process, and we use it here to correct reactions that involve transitions from closed- to open-shell singlet configurations.

2. COMPUTATIONAL METHODS

All stationary points were located by using the UB3LYP functional with the 6-311G*+ level. Transition states were validated to have exactly one negative eigenvalue of the Hessian followed by a minimum energy path (MEP) scan to connect to reactant and product. An open-shell singlet initial guess was used for all calculation. Thermodynamic properties were evaluated at 298.15 K and 1 atm. All DFT calculations were carried out with Jaguar 7.5 package.[39]

After obtaining the reaction paths, single point energy calculation was performed on these geometries for RMP2 and RCCSD(T) with Dunning-type correlation consistent polarized-valence basis sets cc-pVDZ. For PES involving a transition from closed- to open-shell singlet configuration, we also calculated UMP2, UCCSD(T), and GVB-perfect-pairing-(1)-RCI energies with the same basis.

For GVB-PP(1), the bond pair was formed from the orbitals corresponding to the broken bond and then solved self-consistently as a function of bond formation. Starting with this wave function, the correlation consistent CI (CC-CI)[40] would allow single and double excitations from the bond pair × single excitations from the other occupied orbitals on the left × single excitations from the other occupied orbitals on the right. This dissociates to two NO_2 molecules with single excitations from the unpaired electron × single excitations from the remaining occupied orbitals. However we allowed single and double excitations from the bond pair simultaneously with singly excitation from the remaining occupied orbitals to all virtual orbitals (ignoring the limited quadruples in CC-CI). This restricted calculation is referred to as GVB-RCI. Calculations for the case of two NO_2 molecules separated to a N−N distance of 4 Å show that ignoring the restricted quadruple excitations leads to an energy 0.6 kcal/mol higher than the two separating NO_2 molecules with the single−single excitations. The N−N bond scan of N_2O_4 (see Figure 4) shows that it is valid to consider two NO_2 as isolated with 4 Å separation, and we took this point as the reference for all GVB-RCI calculations.

dx.doi.org/10.1021/ja300545e | J. Am. Chem. Soc. 2012, 134, 12970−12978

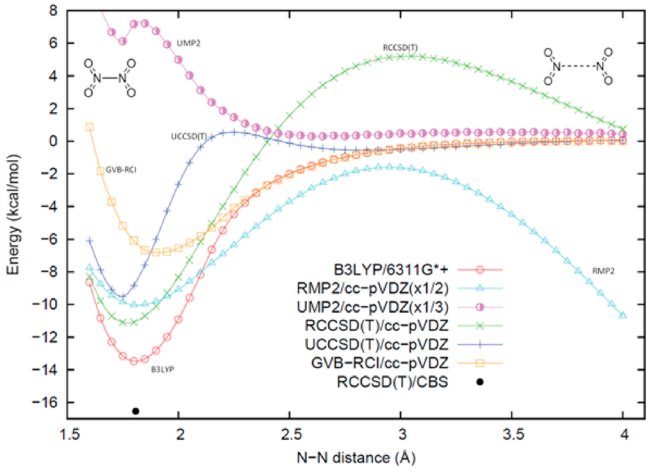

Figure 4. The PES for symmetric dimerization $2NO_2 \rightarrow N_2O_4$. Geometries were obtained from the relaxed N–N bond scan at B3LYP/6311G*+ level. We conclude that there is no barrier, as also found in refs 32 and 35, and consider that the total bond energy of 16.5 kcal/mol from RCCSD(T)/CBS (before ZPE and thermocorrection) is the most reliable.

At stationary points, a further single point RCCSD(T) calculation at cc-pVTZ and cc-pVQZ basis were carried out to extrapolate to the complete basis set (CBS) limit based on Truhlar's formula:[41]

$$E(n) = E_\infty + An^{-\gamma} \quad (7)$$

for RHF and correlation energy, respectively. All three parameters were determined against energies at cc-pVDZ, pVTZ, and pVQZ levels. For RHF, the exponent γ ranges from 2.8 to 2.9 and for CCSD(T) γ is ~2.0 for all cases in this study, comparing values Fast et al. suggested,[42] 3.4 and 2.0. Parameters and energetics for other methods, such as MP2 and CCSD, can be found in Supporting Information.

The reference for all PES is the energy of two isolated NO_2 molecules for all methods except GVB-RCI, as discussed above. CCSD(T) and MP2 calculations were carried out using the NWChem 5.0 package.[43,44] GVB-RCI calculation was carried out by GAMESS[45] via the function of occupation restricted multiple active space.[46] The geometries and orbitals were visualized by Molden[47] and MacMolPlt.[48]

3. RESULTS AND DISCUSSION

Five reaction paths between five intermediates were studied as shown in Scheme 1, with their thermochemical data listed in Table 1. Among all methods used in this study, we considered RCCSD(T)/CBS as the most accurate for bound molecules, and therefore we reported its single point energies in the second column of Table 1. Enthalpy and Gibbs free energy were obtained after the correction of zero point energy (ZPE) and thermodynamics from the B3LYP Hessian, except for TS4 and TS5, for which B3LYP drastically deviates from the ab initio result, where we used the RMP2 geometries and Hessian instead. Geometries and single point energies from other methods are in the Supporting Information. If not otherwise specified, when a barrier height was mentioned, it refers to the single-point energy difference between reactant and TS without ZPE and thermocorrection to match the PES. The discussions of these reactions follow.

3.1. $2NO_2 \rightarrow O_2N\text{-}NO_2$. The PES is shown in Figure 4 for this reaction, which was determined allowing the geometry to relax for each N–N distance between the two NO_2 molecules. UB3LYP leads to a barrierless energy curve for recombination,

Table 1. Thermochemical data of dinitrogen tetroxide isomers and TS geometries. Units in kcal/mol

	B3LYP/ 6311G*+	RCCSD(T)/ CBS	ZPE	ΔH_{298}	ΔG_{298}
$2NO_2$-infinitely separated	0	0	5.5	0	0
$2NO_2$-C_{2v} van der Waals complex	−1.2	−1.6[b]	11.8	−0.6	8.2
N_2O_4	−13.5	−16.5	14.6	−13.9	−1.2
cis-ONO-NO_2	0.6	−5.9	13.4	−4.2	7.6
trans-ONO-NO_2	−1.7	−7.9	13.3	−6.2	5.3
TS1	13.8	12.8	12.1	13.2	25.2
TS2	2.3	0.5	12.5	1.3	13.3
TS3	28.8	29.1	12.8	30.0	42.7
TS4[a]	3.0	−3.1	13.4	−1.8	11.0
TS5[a]	1.4	−2.8	13.8	−1.5	11.9

[a]Geometries and Hessians from RMP2/cc-pVDZ. [b]From UCCSD-(T)/cc-pVTZ.

accompanying a smooth decreasing of spin contamination from S^2 = 1 (half singlet, half triplet) to 0 (closed shell). The electronic bond energy of the N–N bond (ΔE_e) is 13.5 kcal/mol. Including ZPE, the bond energy at 0 K (ΔH_0) becomes 9.9 kcal/mol, consistent with the 10.0 kcal/mol obtained in ref 31 at the same level of theory.

For RCCSD(T)/CBS we find the ΔH_{298} is 13.9 kcal/mol, in very good agreement with experimental values, which range from 13.1,[49] 13.6,[50] to 13.7[51] kcal/mol.

Restricted-wave function-referenced methods, RMP2 and RCCSD(T), lead to a reasonable PES near the equilibrium bond distance. RCCSD(T)/cc-pVDZ leads to a reasonable bond energy of ΔE_e 12.4 kcal/mol, whereas RMP2 overestimates ΔE_e as 24.0 kcal/mol, twice the experimental value. However both methods lead to an unphysical barrier for bond breaking. Such artificial barriers result from the inability of the restricted wave function to dissociate properly and is observed in many bond-breaking processes, such as F–F,[37] B–H, H–F, and H–CH_3.[52]

On the other hand, UMP2 and UCCSD(T) give the correct asymptotic dissociation limit, although UMP2 approaches this limit slowly. However, at shorter distance, these open-shell wave functions do not recover as much correlation energy as do the restricted wave functions. Thus UCCSD(T) still leads to a small barrier artifact for recombination. Furthermore, ΔE_e from UCCSD(T) is 3.6 kcal/mol less than from RCCSD(T). UMP2 is qualitatively wrong, leading to a repulsive curve for recombination (similar behavior was also found in the PES of B–H dissociation).[52]

With this failure of the common ab initio methods, the question is: What is the suitable method to distinguish whether a bond fission reaction is barrierless or not? One quick way to estimate the barrier height is use the RCCSD(T) surface at the recombination side to recover the most correlation energy and then switch to UCCSD(T) along the dissociating surface to avoid the unphysical asymptotic behavior due to the closed-shell reference function. We estimate that the transition from RCCSD(T) to UCCSD(T) takes place at N–N = 2.5 Å, suggesting a negligible barrier for the overall reaction.

A less ad hoc approach would be to use a reference function that dissociates properly to account for the static correlation energy and then to include the dynamic part. GVB-RCI fulfills this requirement, giving a monotonically descending recombination with corrected to ΔE_e 6.8 kcal/mol. Based on the above

dx.doi.org/10.1021/ja300545e | J. Am. Chem. Soc. 2012, 134, 12970–12978

discussions, we conclude that the recombination of two NO_2 into N_2O_4 is barrierless.

3.2. $2NO_2$ → *trans*-ONO-NO_2. All methods find a real barrier for this reaction, as shown in Figure 5. From UB3LYP

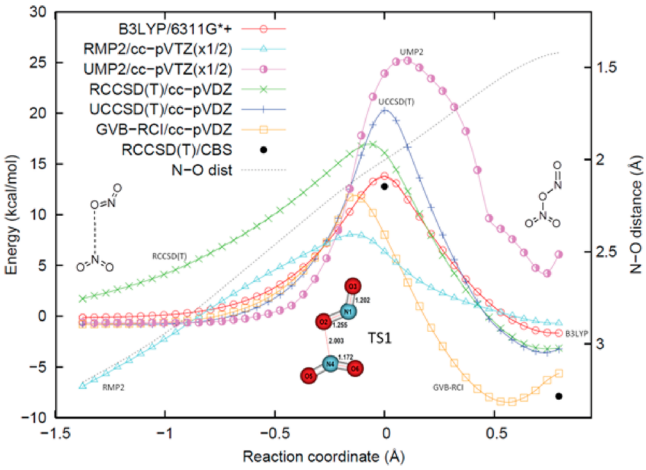

Figure 5. The PES for asymmetric dimerization $2NO_2$ → *trans*-ONO-NO_2. Geometries were obtained from the MEP scan at B3LYP/6311G*+ level. We consider that the barrier of 12.8 kcal/mol from RCCSD(T)/CBS (before ZPE and thermocorrection) is the most reliable.

calculation, the recombination starts from two separating NO_2 molecules with open-shell singlet configuration (S^2 = 1.0), reaches the TS with barrier height 13.8 kcal/mol (S^2 = 0.3) and O−N distance 2.00 Å, and ends up with the closed-shell *trans*-ONO-NO_2 (S^2 = 0). Our result is very different than that of ref 31, which concluded that this recombination is barrierless. However, we found that we could reproduce the barrierless PES with an incorrect closed-shell initial guess. The barrier height given by GVB-RCI is 11.7 kcal/mol, supporting the non-negligible barrier in this reaction. Gadzhiev et al. carried out a multiferfence CAS(26,16) calculation, which gives barrier height 16.6 kcal/mol, similar to our value. Without locating the exact TS, Luo and Chen applied CAS(12e, 9o)/CASPT2 and found a similar barrier height, 17.1 kcal/mol. However these two CAS methods underestimated the ΔE_e, leading to −0.4 and −1.3 kcal/mol, respectively, compared with −4.8 kcal/mol from GVB-RCI (for a different geometry) and −4.9 from RCCSD(T) with the cc-pVDZ basis set, indicating that balanced static and dynamic correlations are important to describe the overall PES. Based on ab initio calculations using the cc-pVDZ basis, RMP2 and RCCSD(T) give consistent bonding energy (ΔE_e = 5.3 kcal/mol for RMP2 and 4.5 kcal/mol for RCCSD(T)), yet they lead to incorrect dissociation limits. On the other hand UMP2 and UCCSD(T) have the correct asymptotic dissociation limit but underestimate the bond energy, similar to the case of $2NO_2$ → N_2O_4. A more realistic PES for recombination could be reconstructed by starting with the dissociation limit of unrestricted methods and switching to restricted ones when the former is higher than the latter. For both MP2 and CCSD(T), the transitions take place before reaching the maximum of the PES, which means RMP2 and RCCSD(T) describe the TS better than UMP2 and UCCSD(T) do. Based on this observation, we consider that the 12.8 kcal/mol barrier height from RCCSD(T)/CBS is the most reliable.

3.3. $2NO_2$ → *cis*-ONO-NO_2. B3LYP calculation leads to the double peaks on the PES shown in Figure 6, with two TS along

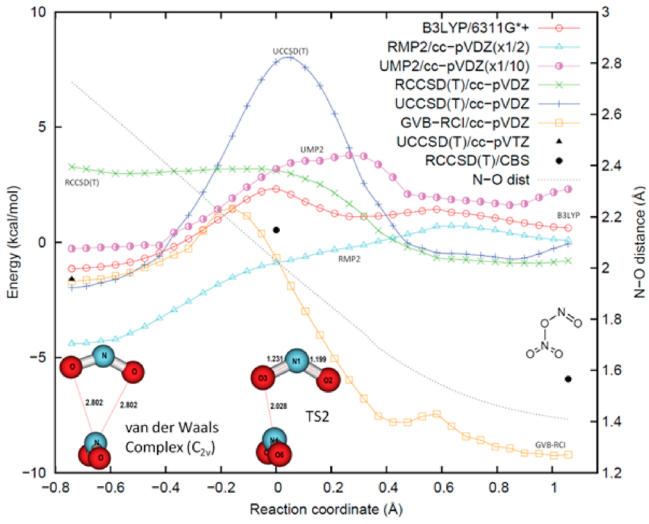

Figure 6. The PES for asymmetric dimerization $2NO_2$ → *cis*-ONO-NO_2. Geometries were obtained from the MEP scan at B3LYP/6311G*+ level. See the text for the interpretation of these results.

the reaction path. The first half of the reaction starts with two NO_2 weakly bonded with each other in C_{2v} symmetry. They approach each other perpendicularly to make a new O−N bond, reach the TS with the O−N bond of 2.03 Å, and end up with the intermediate structure with an O−N bond of 1.75 Å while still keeping the overall perpendicular conformation. The second half of reaction proceeds as the newly formed O−N bond shortens and twists to form a more planar *cis*-ONO-NO_2 (O−N−O−N dihedral angel is 143.26°). The second TS is only 0.3 kcal/mol higher than the intermediate and 0.4 kcal/mol lower after the ZPE correction. This suggests that the second half of the reaction should be considered as barrierless, and the true barrier is located at the first half of the reaction path where two NO_2 start to recombine. GVB-RCI and RCCSD(T)/cc-pVDZ also support that the major barrier for this reaction is at the first half of reaction, with the geometry given in Figure 6.

All methods with correct asymptotic dissociation limits indicate that this recombination has a barrier. The barrier height relative to the van der Waals complex is 3.2 kcal/mol from GVB-RCI and 3.5 kcal/mol from UB3LYP. MP2 is not able to resolve such a low barrier height in the reaction: RMP2 gives an endothermic recombination curve due to the failure of the closed-shell reference at the dissociation limit, and UMP2 exaggerates the barrier by about 10 times. In ref 27, the CAS(26,16) gave a 5.6 kcal/mol barrier, but the recombination was endothermic (5.2 kcal/mol), which might result from the lack of dynamic correlation or from the unbalance of the static correlation at reactant and product side. UCCSD(T)/cc-pVDZ gives a barrier height 10.0 kcal/mol, however if allowed to switch to RCCSD(T)/cc-pVDZ, the barrier height drops to 3.8 kcal/mol, close to B3LYP and GVB-RCI results. RCCSD(T)/CBS gives the TS energy 0.5 kcal/mol higher than two infinitely separated NO_2. For the C_{2v} van der Waals complex, the highest level of theory achieved in this study is UCCSD(T)/cc-pVTZ, giving the binding energy 1.6 kcal/mol. See Supporting Information for the scan of N−N distance of this van der Waals complex. Combing with the TS energy

dx.doi.org/10.1021/ja300545e | J. Am. Chem. Soc. 2012, 134, 12970−12978

from RCCSD(T)/CBS, we conclude that the best number for the barrier height is 2.1 kcal/mol.

3.4. N_2O_4→*trans*-ONO-NO_2. This reaction involves only closed-shell species, so RMP2 and RCCSD(T) are sufficient to describe properly the whole reaction, as shown in Figure 7.

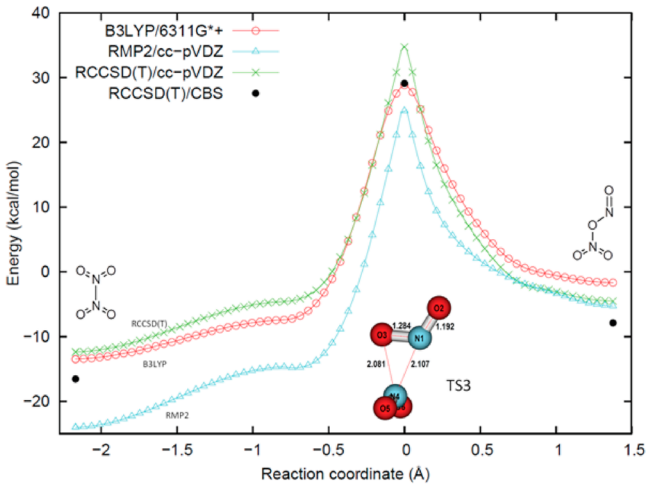

Figure 7. The PES for isomerization of N_2O_4 → *trans*-ONO-NO_2. Geometries were from the MEP scan at B3LYP/6311G*+ level. We consider that the barrier of 45.6 kcal/mol from RCCSD(T)/CBS (before ZPE and thermo correction) is the most reliable.

Based on B3LYP results, two NO_2 are coplanar in the reactant and product but are perpendicular in the TS, consistent with the result from ref 30 but different than that of ref 25, which gave a planar TS in C_{2h}. The B3LYP barrier height is 42.3 kcal/mol.

RMP2 gives barrier 48.9 kcal/mol, and RCCSD(T)/cc-pVDZ gives 47.2 kcal/mol, close to 43.3 kcal/mol from QCISD/6311G*+.[30] RCCSD(T)/CBS gives $\Delta H^{\#}$ 43.9 kcal/mol after ZPE and thermodynamic corrections, as our best estimation of the enthalpic barrier.

3.5. *cis*-ONO-NO_2 → *trans*-ONO-NO_2 and NO^+ Migration in *trans*-ONO-NO_2. The *cis*−*trans* isomerization involves only closed-shell species, and hence we used only the RMP2 and RCCSD(T) methods here. B3LYP gives two TS and one intermediate along the reaction path, which is very different than the PES from ab initio methods, as shown in Figure 8. After the first peak (TS4), B3LYP starts to deviate from ab initio methods drastically: B3LYP gives a stable NO_3^- and NO^+ ionic pair intermediate, whereas in both RMP2 and RCCSD(T), the same geometry is a saddle point (TS5). This disagreement between B3LYP and ab initio methods indicates that B3LYP underestimates the energy of the ionic pair by ∼3 kcal/mol, leading to a wrong PES. This same questionable intermediate was also found with B3LYP in ref 14.

To obtain a more accurate reaction path, we used RMP2/cc-pVDZ to reoptimize TS4 and TS5, followed by a MEP scan at the same level of theory, resulting in two distinct reaction paths, as shown in Figures 9 and 10. Using these RMP2-based geometries, we then calculated RCCSD(T) and B3LYP single point energies. According to these two MEP scans, TS4 is the only TS to connect *cis* and *trans* conformers, while TS5 is the TS for the reaction to exchange NO^+ between oxygen atoms in NO_3^-. Thus we conclude that the enthalpic barrier to convert *cis*- to *trans*-ONO-NO_2 is 2.4 kcal/mol, consistent with the number reported in ref 27, 2.8 kcal/mol. Such a low barrier

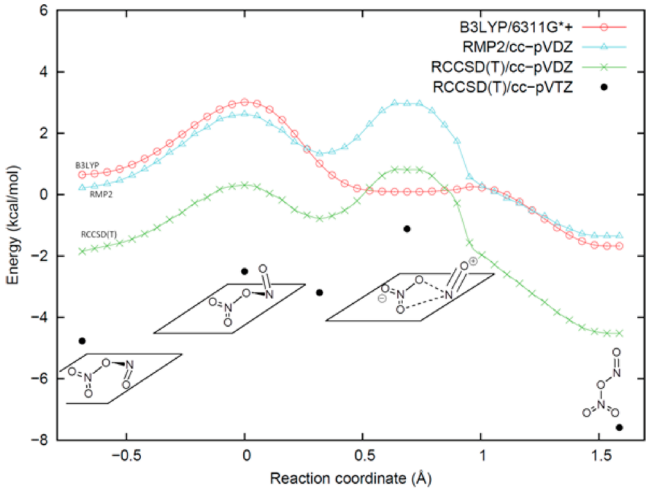

Figure 8. The PES for the reaction *cis*-ONO-NO_2→*trans*-ONO-NO_2. Geometries were obtained from the MEP scan at B3LYP/6311G*+ level. This shows that B3LYP deviates from RMP2 and RCCSD(T) as the reaction proceeds, rendering B3LYP less credible for studying this reaction.

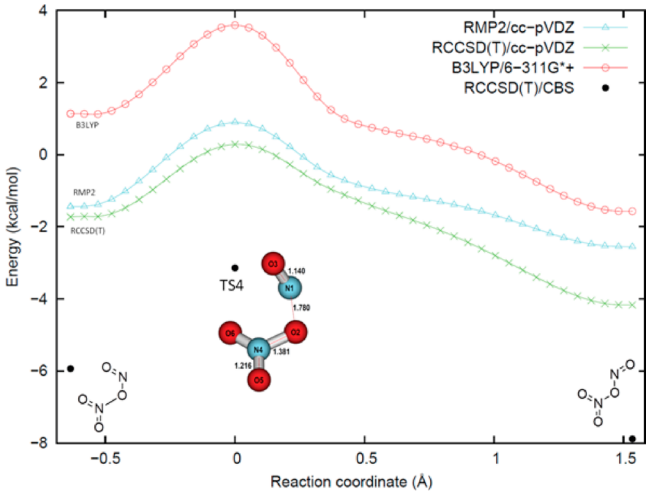

Figure 9. The PES for the reaction *cis*-ONO-NO_2→*trans*-ONO-NO_2. Geometries were obtained from the MEP scan at the RMP2/cc-pVDZ level. We consider that the barrier of 2.8 kcal/mol from RCCSD(T)/CBS (before ZPE and thermocorrection) is the most reliable.

could lead to a fast equilibrium between *cis* and *trans*-ONO-NO_2 at room temperature. The ON^+ group in *trans*-ONO-NO_2 can not only rotate around the same oxygen but also migrate between two oxygen ends of NO_3^- via TS5. This ON-exchange pathway also has a low enthalpic barrier, 4.7 kcal/mol, which explains the rapid self-exchange of oxygen observed in isotopically labeled NO_2, as described in Section 3.7.

3.6. Relation between Barrier Heights and Resonance Structures of NO_2. The richness of NO_2 chemistry derives from the delocalization of the $4a_1$ SOMO, which allows it to form new bonds on either N or O atoms or in various conformations (*cis* or *trans*). Considering the three NO_2 recombination reactions in this study, we find that there is no barrier to form symmetric N_2O_4, a low barrier (2.1 kcal/mol) to form *cis*-ONO-NO_2, and a high barrier (12.8 kcal/mol) to form *trans*-ONO-NO_2.

The trend is similar to what was found in the O−O bond cleavage of ONO-ONO isomers:[26] During the O−O bond

dx.doi.org/10.1021/ja300545e | J. Am. Chem. Soc. 2012, 134, 12970−12978

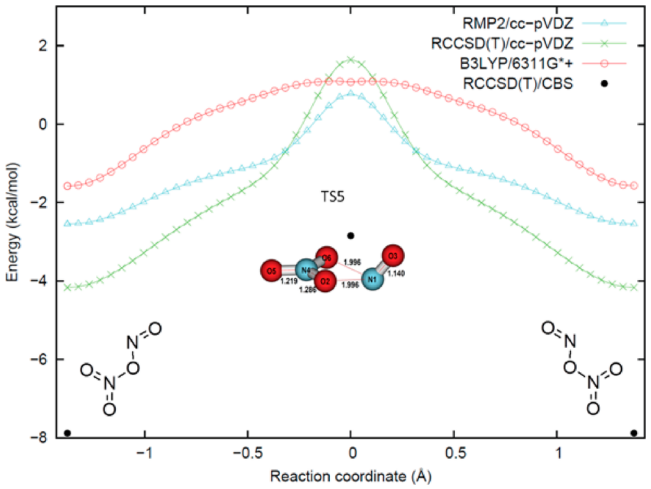

Figure 10. The PES of the reaction *trans*-ONO-NO_2 → $NO^+NO_3^-$ (TS) → *trans*-ONO-NO_2. Geometries were obtained from the MEP scan at RMP2/cc-pVDZ level. We consider that the barrier of 5.1 kcal/mol from RCCSD(T)/CBS(before ZPE and thermocorrection) is the most reliable.

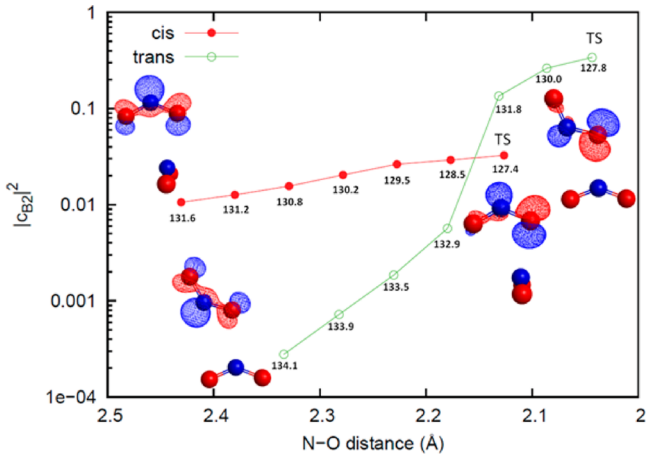

Figure 11. The weighting of B_2 orbital ($|c_{B_2}|^2$) based on the decomposition of GVB orbital $\varphi_{GVB} = c_{A_1}\varphi_{A_1} + c_{B_2}\varphi_{B_2}$ as a function of N–O distance to form *cis*- and *trans*-ONO-NO_2. For *trans*-ONO-NO_2, the much larger $|c_{B_2}|^2$ at TS indicates that there is more $A_1 \rightarrow B_2$ excitation involved and hence a higher barrier. The GVB orbital for both cases at reactant side (mostly A_1) and TS (mixture of A_1 and B_2) is also given. The ONO bond angle is given at each geometry.

cleavage, –ONO group orienting in *cis* conformation of the O–O bond stays in the A_1-like ground state, leading the low barrier to dissociate, while the –ONO group in *trans* conformation dissociates into a B_2-like state, which is 17–25 kcal/mol higher than the A_1 state and raises the barrier by ~15 kcal/mol for each *trans* fragment. In the same language, the formation of *trans*-ONO-NO_2 will excite one of the –ONO fragments to a B_2 state and raise the barrier, whereas the formation of *cis*-ONO-NO_2 can keep –ONO and –NO_2 fragments at the A_1-like state, resulting in a lower barrier.

To examine this idea, a direct and intuitive method to study the state mixing is to project the GVB orbital into the A_1 and B_2-like MO orbitals:

$$\varphi_{GVB} = c_{A_1}\varphi_{A_1} + c_{B_2}\varphi_{B_2}$$

where φ_{A_1} and φ_{B_2} are the MO's of the NO_2 monomer at the same geometry as the dimer. (Although strict C_{2v} symmetry is lost, the shape of MO is maintained if the geometry is not perturbed too much.) By comparing the two coefficients we can quantify the degree of excitation. We plotted the GVB orbitals and their weight of the B_2 component, $|c_{B_2}|^2$, along the reaction coordinate to form *cis*- and *trans*-ONO-NO_2 in Figure 11. To be consistent, the TS for both are taken from GVB-RCI (the peak along the reaction pathway) rather than B3LYP, which are slightly later. To form *cis*-ONO-NO_2, the coefficient of B_2 increases smoothly leading to only 3% B_2 contribution at the TS. On the other hand, to recombine into *trans*-ONO-NO_2, the B_2 coefficient remains low but jumps suddenly at a O–N distance of 2.18 Å leading to 34% contribution from the B_2 orbital at the TS. Since the A_1-like orbital does not overlap well with the free radical coming from the *trans* position, it must hybridize with the B_2 orbital (equivalent to partial excitation) to enhance the overlap required for better bonding, resulting in a higher barrier. To form sym-N_2O_4, by symmetry, there is no B_2 orbital involved to form the N–N bond and therefore no extra excitation, resulting in no barrier for the recombination.

3.7. Role of Asymmetric Dimer ONONO$_2$ in NO$_2$ Hydrolysis and Oxygen Exchange in NO$_2$ Gas. Finlayson-Pitts et al.[7] proposed that to react with water, N_2O_4 symmetric dimer must isomerize to the asymmetric form, ONO-NO_2. Pimental et al.[30] studied the reaction paths with the B3LYP functional and concluded that to form *trans*-ONO-NO_2 via the isomerization from symmetric N_2O_4 there had to be a high barrier (60 kcal/mol) in the gas phase, and the reaction was enthalpically barrierless via asymmetric dimerization from NO_2 monomers. However, we find that both reaction paths to form *trans*-ONO-NO_2 have considerable enthalpic barriers (13.2 kcal/mol for dimerization and 43.9 kcal/mol for isomerization).

On the other hand, we confirmed the two-step reaction path to form *trans*-ONO-NO_2 with a much lower barrier: two NO_2 monomers first dimerize to form *cis*-ONO-NO_2, which then converts to *trans*-ONO-NO_2. Enthalpic barriers for both reactions are less than 3 kcal/mol, and the rate-limiting step is to bring two NO_2 monomers to form *cis*-ONO-NO_2, which has the free energy barrier of 13.3 kcal/mol. Both isomers are much more reactive toward water than the symmetric N_2O_4.[5,29] Due to low enthalpic barriers to form these asymmetric dimers, their formation rate would be mostly determined by how these asymmetric dimers are stabilized. Because of their high polarity (3.45D for *cis* and 2.96D for *trans* at B3LYP/6311G*+ level), asymmetric dimers would likely be stabilized by polar chemical bonds on the surface of a reactor or glass wool, leading to a higher formation rate and concentration on the surface.

The oxygen-exchange reaction is observed experimentally in the isotopically labeled NO_2, i.e.,

$$N^{16}O_2 + N^{18}O_2 \rightarrow 2N^{16}O^{18}O$$

The gas-phase reaction was found to be second order and has a rate constant of $3.0 \pm 1.0 \times 10^6$ L mol^{-1} s^{-1} at 25 °C.[54] We propose that the oxygen-exchange step is via TS5, where NO^+ dissociates from NO_3^- in *trans*-ONO-NO_2 and migrates to the other oxygen. Given reaction barrier heights, the exchange rate is limited by the formation of *cis*-ONO-NO_2 (TS2). Based on transition-state theory and assuming fast equilibrium between isotopically different trans-$ONONO_2$, the theoretical exchange rate constant is 1.8×10^4 L mol^{-1} s^{-1} at 25 °C, corresponding

dx.doi.org/10.1021/ja300545e | J. Am. Chem. Soc. 2012, 134, 12970–12978

to ∼3 kcal/mol difference in free energy compared to the experimental rate. However the experimental exchange rate was found to depend on the surface area of reactor (3.0×10^6 L mol^{-1} s^{-1} for $S/V = 4.0$ cm^{-1} and 1×10^6 L mol^{-1} s^{-1} for $S/V = 0.48$ cm^{-1}),[54] and such a heterogeneous effect is not the topic in this study and not considered here.

Molecular dynamics with MP2 and B3LYP have been applied to study the hydrolysis of NO_2, and their performance was examined in this study. MP2 has been widely applied as a reliable method for MD simulation because that it provides analytic gradient and includes van der Waals interaction for closed-shell system. However in a system in which the transition between closed- and open-shells is important, like the formation of asymmetric ONO-NO_2 in NO_2 hydrolysis, neither RMP2 nor UMP2 is able to give a satisfactory PES. On the other hand, the B3LYP functional leads to a reasonable PES for reactions 1−4 (Sections 3.1−3.4) in this study. However a proper open-shell initial guess is necessary, otherwise the PES will bias to the side of closed-shell species.

4. CONCLUSION

We studied the reaction path from NO_2 monomers to symmetric N_2O_4, *cis*-ONO-NO_2 and *trans*-ONO-NO_2, plus the isomerization of N_2O_4 to *trans*-ONO-NO_2 and the *cis*−*trans* conversion of ONO-NO_2. We examined several ab initio methods (MP2, CCSD(T) and GVB-RCI) and DFT(B3LYP). For N_2O_4, RCCSD(T)/CBS gives N−N bond energy (ΔH_{298}) of 13.9 kcal/mol, in very good agreement with experimental values ranging from 13.1 to 13.7 kcal/mol. We assume that this level also gives reliable energetics for other species. To study recombinations of NO_2 monomers involving a transition from open- to closed-shell, GVB-RCI is superior to unrestricted-based correlation methods, such as UMP2 and UCCSD(T), even though the latter two also have correct asymptotic behavior.

RCCSD(T)/CBS gives a barrier height of 2.1 kcal/mol to form *cis*-ONO-NO_2 and of 12.8 kcal/mol to form *trans*-ONO-NO_2. The existence and the height of both barriers are well supported by the PES from GVB-RCI.

For reactions involving no open-shell species, RCCSD(T) and RMP2 performed similarly. From RCCSD(T)/cc-pVTZ, the enthalpic barrier for N_2O_4 isomerizing to *trans*-ONO-NO_2 is 43.9 kcal/mol. This high barrier excludes the possibility that such an isomerization plays a significant role in gas-phase hydrolysis of NO_2. A much more favored path is to form *cis*-ONO-NO_2 first, then convert to *trans*-ONO-NO_2 with an enthalpic barrier in 2.4 kcal/mol.

To analyze the conformation-dependent state selectivity we developed an orbital-based method by projecting a GVB orbital onto the MO of a NO_2 monomer and validated that the B_2 orbital plays an important role in the bond formation in *trans* orientation. This study helps elucidate several experimental results, including NO_2 hydrolysis and the oxygen-exchange rate in isotopically labeled NO_2 gas.

■ ASSOCIATED CONTENT

Supporting Information

Scan of N−N distance of C_{2v} van der Waals complex, atomic coordinates of all intermediates and TS shown in this study. This material is available free of charge via the Internet at http://pubs.acs.org.

■ AUTHOR INFORMATION

Corresponding Author

wag@wag.caltech.edu

Notes

The authors declare no competing financial interest.

■ ACKNOWLEDGMENTS

This research was supported by an ARO-MURI grant (W911NF-08-1-0124, Ralph Anthenien). The computational facility was funded by DURIP grants from ARO and ONR.

■ REFERENCES

(1) Addison, C. C. *Chem. Rev.* **1980**, *80* (1), 21−39.
(2) Nonnenberg, C.; Frank, I.; Klapotke, T. M. *Angew. Chem.-Int. Ed.* **2004**, *43* (35), 4585−4589.
(3) Sander, S. P.; Golden, D. M.; Kurylo, M. J.; Moortgat, G. K.; Wine, P. H.; Ravishankara, A. R.; Kolb, C. E.; Molina, M. J.; Finlayson-Pitts, B. J.; Huie, R. E.; Orkin, V. L.; Friedl, R. R.; Keller-Rudek, H. *Chemical kinetics and photochemical data for use in atmospheric studies: evaluation number 15*; Jet Propulsion Laboratory, California Institute of Technology: Pasadena, CA, 2006.
(4) Raff, J. D.; Njegic, B.; Chang, W. L.; Gordon, M. S.; Dabdub, D.; Gerber, R. B.; Finlayson-Pitts, B. J. *Proc. Natl. Acad. Sci. U.S.A.* **2009**, *106* (33), 13647−13654.
(5) Njegic, B.; Raff, J. D.; Finlayson-Pitts, B. J.; Gordon, M. S.; Gerber, R. B. *J. Phys. Chem. A* **2010**, *114* (13), 4609−4618.
(6) Koda, S.; Yoshikawa, K.; Okada, J.; Akita, K. *Environ. Sci. Technol.* **1985**, *19* (3), 262−264.
(7) Finlayson-Pitts, B. J.; Wingen, L. M.; Sumner, A. L.; Syomin, D.; Ramazan, K. A. *Phys. Chem. Chem. Phys.* **2003**, *5* (2), 223−242.
(8) Bent, H. A. *Inorg. Chem.* **1963**, *2* (4), 747−752.
(9) Liu, R. F.; Zhou, X. F. *J. Phys. Chem.* **1993**, *97* (17), 4413−4415.
(10) Stirling, A.; Papai, I.; Mink, J.; Salahub, D. R. *J. Chem. Phys.* **1994**, *100* (4), 2910−2923.
(11) McKee, M. L. *J. Am. Chem. Soc.* **1995**, *117* (5), 1629−1637.
(12) Ahlrichs, R.; Keil, F. *J. Am. Chem. Soc.* **1974**, *96* (25), 7615−7620.
(13) Wang, X. F.; Qin, Q. Z.; Fan, K. N. *Theochem J. Mol. Struct.* **1998**, *432* (1), 55−62.
(14) Zakharov, I. I.; Kolbasin, A. I.; Zakharova, O. I.; Kravchenko, I. V.; Dyshlovoi, V. I. *Theor. Exp. Chem.* **2008**, *44* (1), 26−31.
(15) Agnew, S. F.; Swanson, B. I.; Jones, L. H.; Mills, R. L. *J. Phys. Chem.* **1985**, *89* (9), 1678−1682.
(16) Jones, L. H.; Swanson, B. I.; Agnew, S. F. *J. Chem. Phys.* **1985**, *82* (9), 4389−4390.
(17) Givan, A.; Loewenschuss, A. *J. Chem. Phys.* **1989**, *90* (11), 6135−6142.
(18) Givan, A.; Loewenschuss, A. *J. Chem. Phys.* **1989**, *91* (8), 5126−5127.
(19) Givan, A.; Loewenschuss, A. *J. Chem. Phys.* **1991**, *94* (11), 7562−7563.
(20) Fateley, W. G.; Bent, H. A.; Crawford, B. *J. Chem. Phys.* **1959**, *31* (1), 204−217.
(21) Hisatsune, I. C.; Devlin, J. P.; Wada, Y. *J. Chem. Phys.* **1960**, *33* (3), 714−719.
(22) Stlouis, R. V.; Crawford, B. *J. Chem. Phys.* **1965**, *42* (3), 857−864.
(23) Bolduan, F.; Jodl, H. J.; Loewenschuss, A. *J. Chem. Phys.* **1984**, *80* (5), 1739−1743.
(24) Beckers, H.; Zeng, X. Q.; Willner, H. *Chem.—Eur. J.* **2010**, *16* (5), 1506−1520.
(25) Gadzhiev, O. B.; Ignatov, S. K.; Razuvaev, A. G.; Masunov, A. E. *J. Phys. Chem. A* **2009**, *113* (32), 9092−9101.
(26) Olson, L. P.; Kuwata, K. T.; Bartberger, M. D.; Houk, K. N. *J. Am. Chem. Soc.* **2002**, *124* (32), 9469−9475.
(27) Gadzhiev, O. B.; Ignatov, S. K.; Gangopadhyay, S.; Masunov, A. E.; Petrov, A. I. *J. Chem. Theory Comput.* **2011**, *7* (7), 2021−2024.

(28) Chou, A.; Li, Z. R.; Tao, F. M. *J. Phys. Chem. A* **1999**, *103* (39), 7848−7855.
(29) Zhu, R. S.; Lai, K.-Y.; Lin, M. C. *J. Phys. Chem. A* **2012**, *116* (18), 4466−4472.
(30) Pimentel, A. S.; Lima, F. C. A.; da Silva, A. B. F. *J. Phys. Chem. A* **2007**, *111* (15), 2913−2920.
(31) Pimentel, A. S.; Lima, F. C. A.; da Silva, A. B. F. *Chem. Phys. Lett.* **2007**, *436* (1−3), 47−50.
(32) Luo, G. F.; Chen, X. B. *J. Phys. Chem. Lett.* **2012**, *3* (9), 1147−1153.
(33) Miller, Y.; Finlayson-Pitts, B. J.; Gerber, R. B. *J. Am. Chem. Soc.* **2009**, *131* (34), 12180−12185.
(34) Medeiros, D. D.; Pimentel, A. S. *J. Phys. Chem. A* **2011**, *115* (24), 6357−6365.
(35) Li, Y. M. *J. Chem. Phys.* **2007**, *127* (20), 204502.
(36) Ornellas, F. R.; Resende, S. M.; Machado, F. B. C.; Roberto-Neto, O. *J. Chem. Phys.* **2003**, *118* (9), 4060−4065.
(37) Bartlett, R. J.; Musial, M. *Rev. Mod. Phys.* **2007**, *79* (1), 291−352.
(38) Ellison, G. B.; Herbert, J. M.; McCoy, A. B.; Stanton, J. F.; Szalay, P. G. *J. Phys. Chem. A* **2004**, *108* (38), 7639−7642.
(39) *Jaguar*; Schrodinger, LLC: New York, NY, 2007.
(40) Carter, E. A.; Goddard, W. A. *J. Chem. Phys.* **1988**, *88* (5), 3132−3140.
(41) Truhlar, D. G. *Chem. Phys. Lett.* **1998**, *294* (1−3), 45−48.
(42) Fast, P. L.; Sanchez, M. L.; Truhlar, D. G. *J. Chem. Phys.* **1999**, *111* (7), 2921−2926.
(43) Valiev, M.; Bylaska, E. J.; Govind, N.; Kowalski, K.; Straatsma, T. P.; Van Dam, H. J. J.; Wang, D.; Nieplocha, J.; Apra, E.; Windus, T. L.; de Jong, W. *Comput. Phys. Commun.* **2010**, *181* (9), 1477−1489.
(44) Hirata, S. *J. Phys. Chem. A* **2003**, *107* (46), 9887−9897.
(45) Schmidt, M. W.; Baldridge, K. K.; Boatz, J. A.; Elbert, S. T.; Gordon, M. S.; Jensen, J. H.; Koseki, S.; Matsunaga, N.; Nguyen, K. A.; Su, S. J.; Windus, T. L.; Dupuis, M.; Montgomery, J. A. *J. Comput. Chem.* **1993**, *14* (11), 1347−1363.
(46) Ivanic, J. *J. Chem. Phys.* **2003**, *119* (18), 9364−9376.
(47) Schaftenaar, G.; Noordik, J. H. *J. Comput.-Aided Mol. Des.* **2000**, *14* (2), 123−134.
(48) Bode, B. M.; Gordon, M. S. *J. Mol. Graph.* **1998**, *16* (3), 133−+.
(49) Guttman, A.; Penner, S. S. *J. Chem. Phys.* **1962**, *36* (1), 8−99.
(50) Hisatsune, I. *J. Phys. Chem.* **1961**, *65* (12), 2249−2253.
(51) Giauque, W. F.; Kemp, J. D. *J. Chem. Phys.* **1938**, *6* (1), 40−52.
(52) Dutta, A.; Sherrill, C. D. *J. Chem. Phys.* **2003**, *118* (4), 1610−1619.
(53) Lai, K. Y.; Zhu, R. S.; Lin, M. C. *Chem. Phys. Lett.* **2012**, *537*, 33−37.
(54) Sharma, H. D.; Jervis, R. E.; Wong, K. Y. *J. Phys. Chem.* **1970**, *74* (4), 923−933.